**Neuron, volume 52**

## Supplemental Data

# A Central Source of Movement Variability

**Mark M. Churchland, Afsheen Afshar, and Krishna V. Shenoy**

***Supplemental figures***

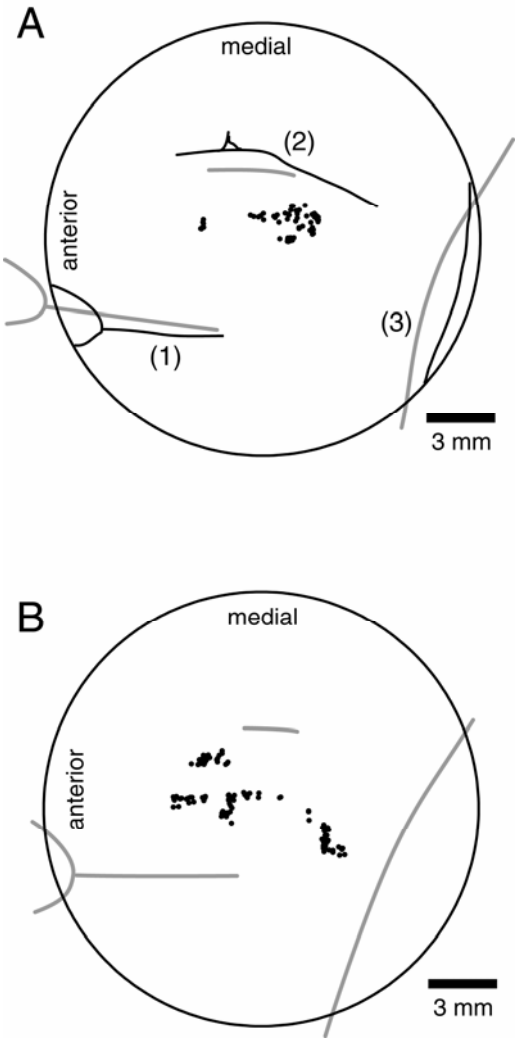


***Figure S1.*** Locations of recording sites. ***A***. Recording sites (black dots, one per neuron) for monkey A. The large circle outlines the limits of the implanted cylinder. Grey lines give the locations, inferred from MRI, of (1) the spur of the arcuate sulcus, (2) the

precentral dimple, and (3) the central sulcus. Black lines give the actual locations, measured at autopsy. A small amount (0-0.3mm) of 'jitter' has been added to the locations of the black dots to make it clear when multiple recordings were made from the same AP location. ***B***. Similar illustration, but for monkey B. This monkey is still actively involved in experiments, so landmarks are estimated solely by MRI.

In making these penetrations, our intent was to record from neurons in caudal PMd and in M1 that exhibited delay-period 'preparatory' activity related to movements of the arm. We avoided sites in rostral PMd, from which eye movements can be evoked (Fujii et al., 2000) and which projects less densely to both M1 and the spinal cord than does caudal PMd (Dum and Strick, 2005). We also recorded only a few sites from the deeper portions of M1 (i.e., in the sulcus below the cortical surface) where delay-period activity was less common. Thus, most penetrations were in caudal PMd near the M1/PMd 'border' and in the adjacent portion of M1. There was a non-significant tendency for both the impact of instructed speed, and the strength of trial-by-trial correlations, to be weaker at more rostral sites.

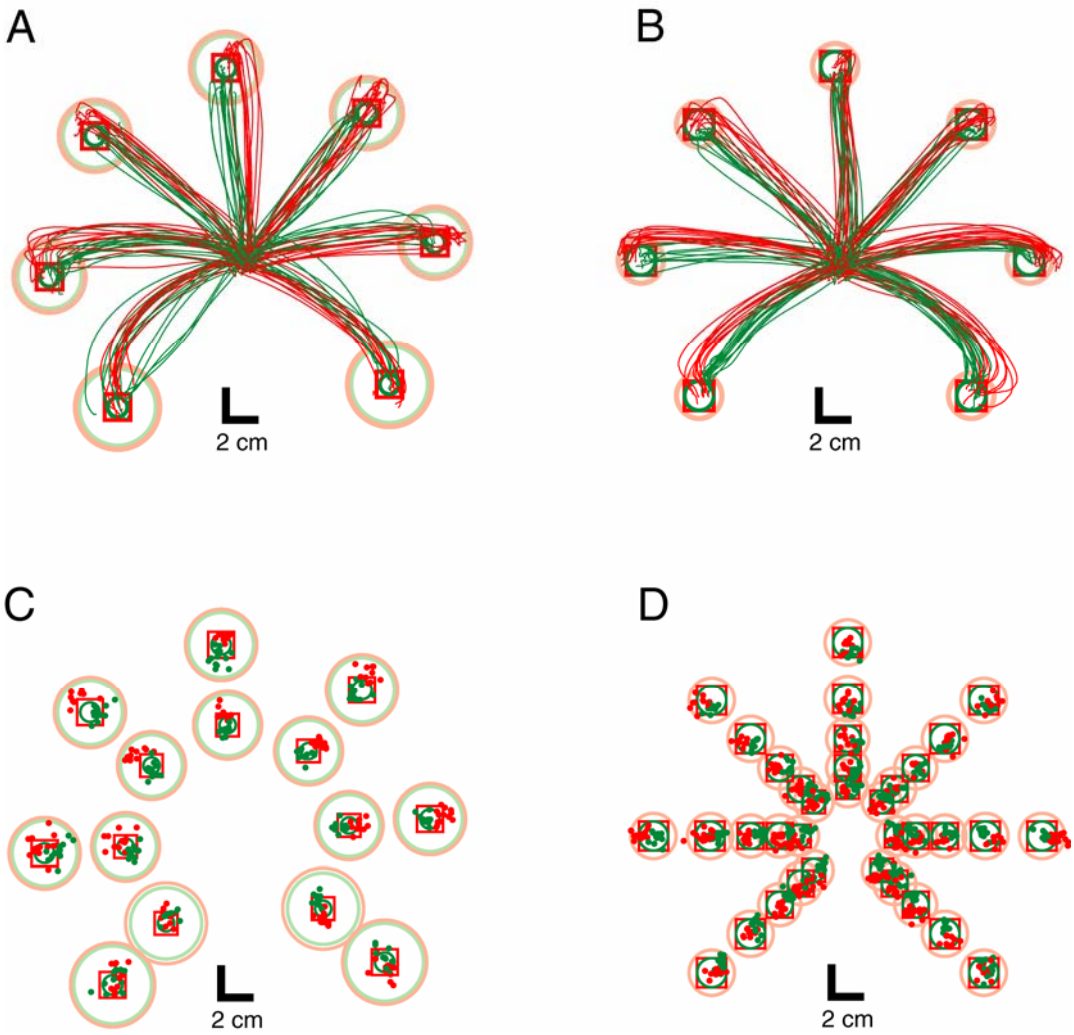


***Figure S2.*** Reach trajectories and endpoints. Data for monkeys A and B are plotted in the left and right panels respectively Red and green traces/symbols plot data for 'fast' and 'slow' reaches to red and green targets. So as to give a correct indication of performance, data are plotted for all saved trials, including occasional failures. Data for monkey A are from a representative recording session (neuron A35). Monkey B was tested using both a 'direction series' (7 directions / 2 distances) and a 'distance series'. For this reason, the data shown are from a special session devoted to thoroughly documenting behavior for all directions/distances. ***A.*** Reach trajectories for monkey A

for the more distant (12 cm) targets. Target locations/dimensions for the seven reach directions are shown by the solid red squares and green circles. The larger light red/green circles plot the acceptance windows for reach endpoint (these were slightly more forgiving for the fast reaches). Reach trajectories are plotted from the time of the go cue until 50 ms after the target was touched. ***B.*** Similar plot for monkey B. Endpoint accuracy was more tightly enforced than for monkey A and was the same for red and green targets (light red circles plot the acceptance windows). ***C.*** Reach endpoints for all directions and distances for monkey A (same dataset as in panel *A*). Reach endpoints were computed 50 ms after the reach ended (i.e., the online estimate of velocity fell to near-zero). Results were essentially identical 200 ms after the reach ended (not shown). ***D.*** Similar plot but for monkey B (same dataset as in panel *B*).

***Supplemental analysis***

*Simulation results*

For the neural recordings, the trial-by-trial slope of firing rate versus peak velocity was, on average, about half the predicted-slope. Perhaps surprisingly, this was also true for the EMG data. To identify factors that could result in a ratio less than unity, we generated artificial data and analyzed it as in figure 5*D*. Simulations assumed that behavioral variability could result from either movement preparation or from online noise. Individual neurons could be tuned either to the planned peak velocity *per se* or to some factor that correlates with peak velocity. In the latter case, the way in which firing rate varied across instructed speeds imperfectly predicted the way in which it varied across within-condition velocity fluctuations. On each trial, the 'measured' neural

response was a noisy estimate (drawn from a Poisson distribution) of the 'actual' firing rate, the latter determined by the 'actual' planned velocity.

Three main points are made by the simulations. First, Poisson spiking statistics did not reduce the trial-by-trial slopes (variability along the y-axis does not, on average, change the slope of a regression). There was nevertheless a slight reduction in the average slope-ratio (trial-by-trial versus predicted). This was due to variability in the estimate of the predicted slope, resulting from the noisy spiking statistics and the finite trial count. Such variability 'smears' the relationship between the trial-by-trial and predicted slopes and reduces the slope-ratio after binning as in figure 5*D* (and similarly reduces the slope of a meta-regression, as in figure 7). However, this effect was small when using 15 simulated trials/condition: a mean slope-ratio of 0.9, rather than unity. As an aside, anti-correlation among similarly-tuned neurons (e.g., generating the same movement plan using different sets of activity on different trials) had a similarly modest impact the slope ratio. One might have thought that additional neural variability (beyond that ascribable to fluctuations in motor planning) would dramatically reduce the slope-ratio, but this is not the case.

Second, when behavioral variability was due in equal part to plan variability and online variability, the mean slope ratio was 0.44. Thus, our experimental results (slope ratio of 0.47) can be explained by assuming that half of the observed behavioral variability arises from the motor preparation stage, and half from the execution stage.

Third, when the factor for which neurons were tuned was imperfectly correlated with peak velocity (*r* of 0.46), the mean slope-ratio was 0.46, even when *all* behavioral variability was due to preparatory variability. This is because the predicted slope is

estimated using the (now faulty) assumption that 'tuning' for instructed speed reflects tuning for peak velocity. Thus, our experimental results could be obtained even if motor preparation were the *sole* source of behavioral variability, if we assume that the observed 'tuning' for instructed-speed reflects sensitivity to something that merely correlates with peak velocity (e.g. peak acceleration, average velocity, peak muscle contraction, degree of co-contraction, movement duration, etc.). In summary, given reasonable assumptions, a slope-ratio of ~0.5 implies that at least half the behavioral variability arises before execution. Assuming that the measured 'tuning' for instructed speed does not truly reflect tuning for peak velocity (something that is almost certainly the case) the proportion will be higher.

*Simulation methods*

Simulations assumed that each neuron is tuned for some 'factor X' that is statistically related to the peak velocity of the planned reach. Thus, $\overline{X}_n$, the mean value across trials for a given neuron, *n*, is assumed to differ between instructed speeds (e.g., most neurons will exhibit 'tuning' for instructed speed). However, this relationship may differ from that expected given the mean peak velocities, $\overline{V}^{\text{fast}}$ and $\overline{V}^{\text{slow}}$. This is captured by drawing values from a normal distribution:

$$\begin{aligned} \overline{X}_n^{\text{fast}} &\sim N\left(\overline{V}^{\text{fast}}, \sigma_X\right) \\ \overline{X}_n^{\text{slow}} &\sim N\left(\overline{V}^{\text{slow}}, \sigma_X\right) \end{aligned} \qquad \text{eqn. 1}$$

If $\sigma_x = 0$, then factor X is simply peak velocity. Otherwise factor X is something that varies with instructed speed, but correlates imperfectly with peak velocity. For

example, factor X could be the degree of planned co-contraction, and $\overline{X}_n^{\text{fast}}$ would then be the typical co-contraction in the instructed-fast condition.

The mean peak velocities, $\overline{V}^{\text{fast}}$ and $\overline{V}^{\text{slow}}$, were set to 60 and 100°/s. For each trial we draw a *planned* peak velocity, *V*, from a normal distribution, centered on the mean peak velocity for the relevant instructed speed (fast or slow):

$$V(trial) \sim N\left(\overline{V}^{\text{instructed speed}}, \sigma_{plan}\right) \qquad \text{eqn. 2}$$

with $\sigma_{plan}$ = 8°/s. The value of factor *X* on each trial is biased by the planned velocity, with some additional variability:

$$X_n(trial) \sim N\left(\overline{X}_n^{\text{instructed speed}} + (V(trial) - \overline{V}^{\text{instructed speed}}), \sigma_X\right) \quad \text{eqn. 3}$$

using the same value, $\sigma_X$, as was used in equation 1. Thus, with $\sigma_X$ = 0, factor X correlates perfectly with the planned peak velocity, both across instructed speeds and across trials. With $\sigma_X$ > 0, the relationship is imperfect in both cases.

Each neuron was assigned a random gain of tuning, $g_n$, with mean zero and standard deviation one. The underlying spike rate, $\mu_n$, on a given trial was

$$\mu_n(trial) = b_n + g \cdot X_n(trial) \qquad \text{eqn. 4}$$

where $b_n$ is the baseline firing rate. For each neuron this was set so that the mean firing rate in the instructed slow condition was 30 spikes/s. On each trial, the observed spike count, *S*, was drawn from:

$$S_n(trial) \sim Poisson\left(\mu_n(trial)\right) \qquad \text{eqn. 5}$$

Lastly, we assumed that the *actual* peak reach velocity, *V'*, is influenced by online noise:

$$V'(trial) \sim N\left(V(trial), \sigma_{online}\right) \qquad \text{eqn. 6}$$

For each neuron, we simulated 15 trials per instructed speed, and computed the predicted slope:

$$\frac{\sum_{\text{instructed fast trials}} S_n(trial) - \sum_{\text{instructed slow trials}} S_n(trial)}{\sum_{\text{instructed fast trials}} V'(trial) - \sum_{\text{instructed slow trials}} V'(trial)} \qquad \text{eqn. 7}$$

This was done for 5000 simulated neurons. Data were then analyzed as in figure 5*D* (analysis as in figure 7 produced similar results). Simulations were run with different values of the parameters $\sigma_X$ and $\sigma_{online}$. With $\sigma_X = 0$ and $\sigma_{online} = 0$, the mean slope-ratio was 0.9. With $\sigma_X = 0$ and $\sigma_{online} = \sigma_{plan}$, the mean slope-ratio was 0.44. Finally, we set $\sigma_{online} = 0$ and $\sigma_X = 30$ (75% of the mean velocity difference between fast and slow reaches). This led to an overall correlation of 0.47 between factor X and the planned velocity (including trials for both instructed speeds). The mean slope-ratio was also 0.47, even though there was no contribution of online noise.

***Supplemental references***

Dum, R.P., and Strick, P.L. (2005). Frontal lobe inputs to the digit representations of the motor areas on the lateral surface of the hemisphere. J. Neurosci. 25, 1375–1386.

Fujii, N., Mushiake, H., and Tanji, J. (2000). Rostrocaudal distinction of the dorsal premotor area based on oculomotor involvement. J. Neurophysiol. 83, 1764–1769.